Supplements

Figures in supplementary material

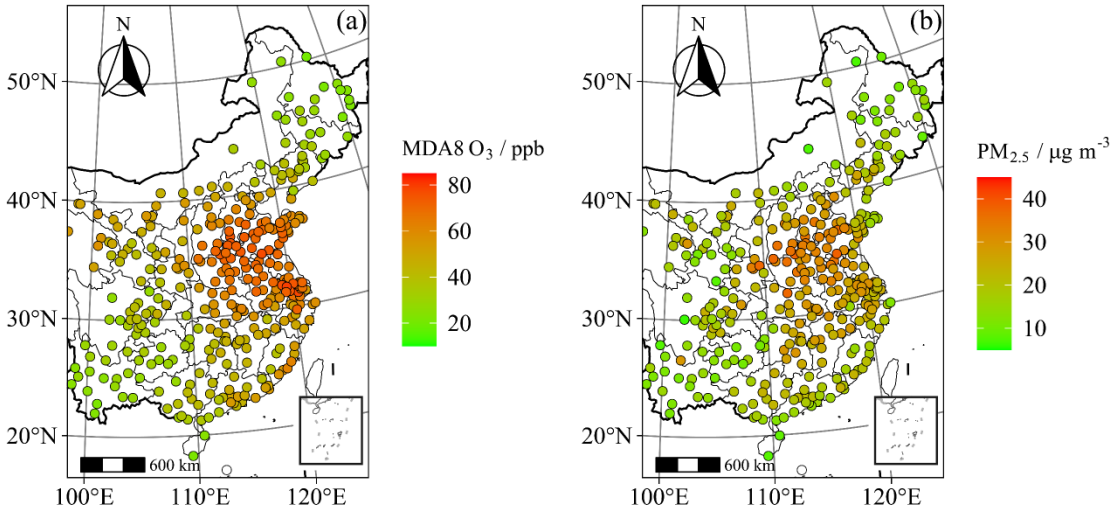

Fig. S1. (a) The daily maximum 8-hour average ozone (MDA8) and **(b)** daily average $PM_{2.5}$ in September 2020 at individual cities of the surface network operated by the China MEE. The data points are averages over the entire observation period (0901-0920).

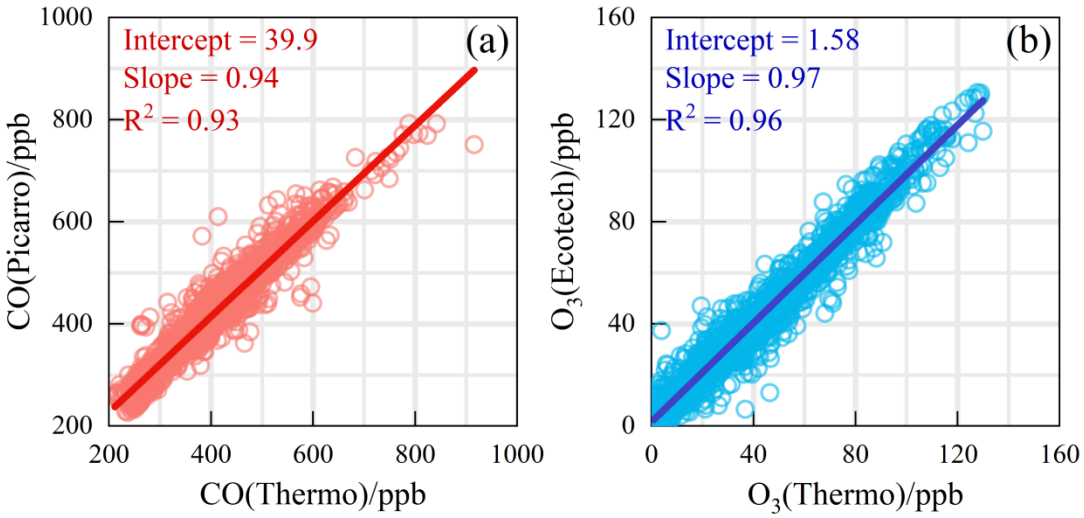

Fig. S2. The comparison results between different technologies. **(a)** CO measurements by Thermo 48i and Picarro-G2401. **(b)** O_3 measurements by Thermo 49i and Ecotech EC9810B.

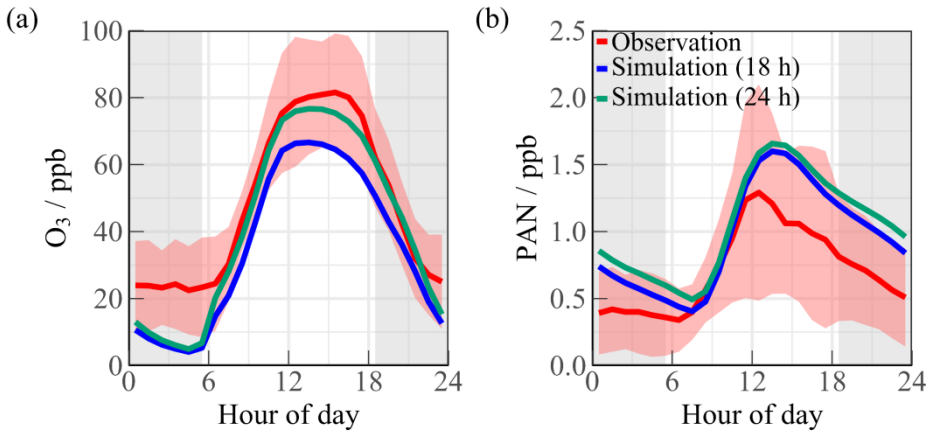

Fig. S3. The comparison results of **(a)** ozone and **(b)** PAN between simulation and observation.

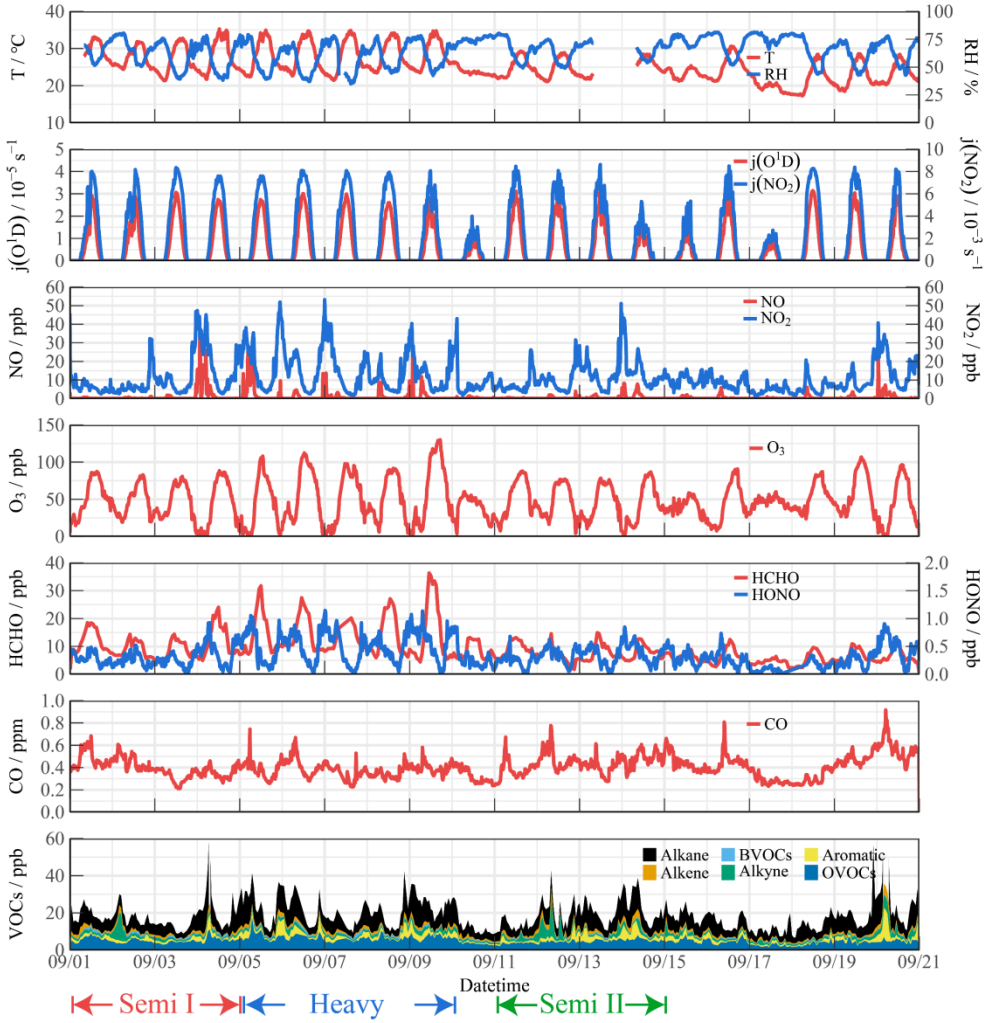

Fig. S4. Time series of observed meteorological and chemical parameters during the campaign. The entire ozone pollution is divided into three continuous periods according to pollution level (Semi I, Heavy, and Semi II).

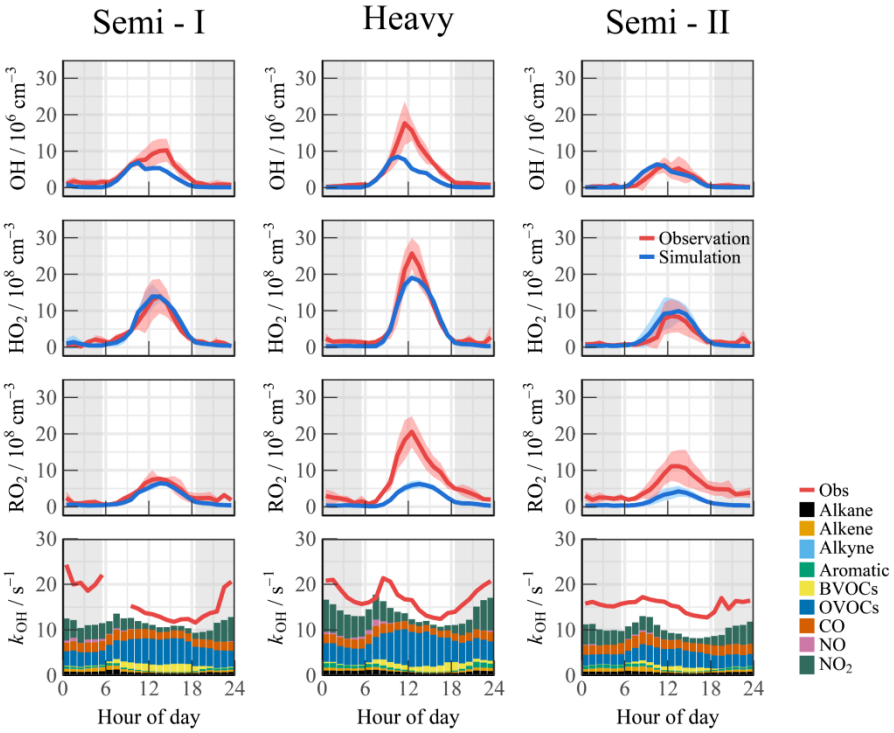

Fig. S5. Diurnal profiles of the observed and modelled OH, HO_2, RO_2 and k_{OH} in different episodes (Semi I, Heavy, and Semi II). The coloured shadows denote the 25 and 75% percentiles. The grey areas denote nighttime.

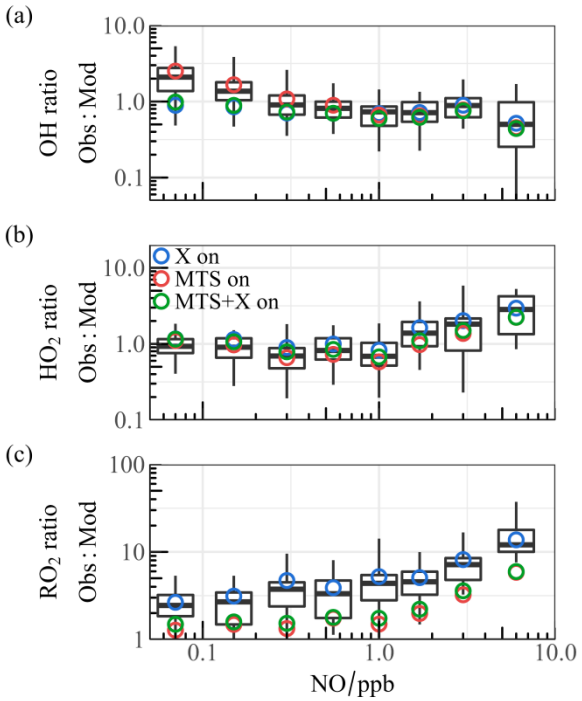

Fig. S6. The relationship between NO and the "observation-to-simulation" ratios for **(a)** OH, **(b)** HO_2, and **(c)** RO_2 concentrations. Boxplot diagrams illustrate the dataset's minimum, 25th percentile, median, 75th percentile, and maximum values. The circles represent median values by different mechanisms added to the base model within various ranges.

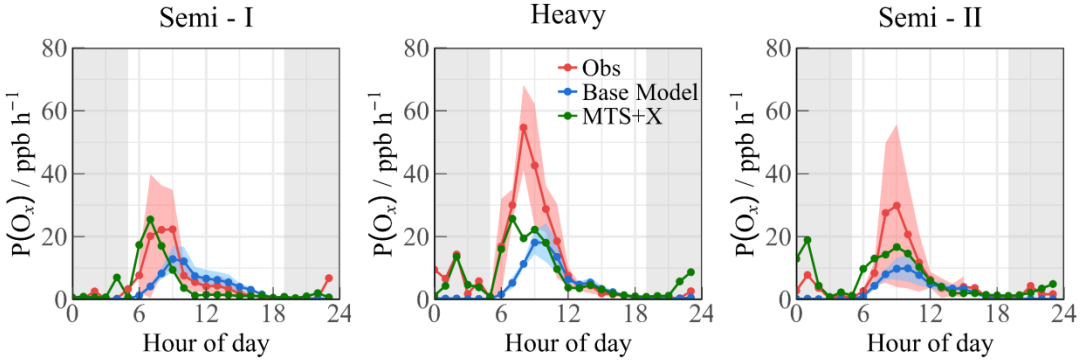

Fig. S7. The P(Ox) values that calculated by different radical values (Scenario 1: by the observed values; Scenario 2: by the base model values. Scenario 3: by both considering X mechanism and the influence of monoterpenes under the base model). The grey areas denote nighttime.

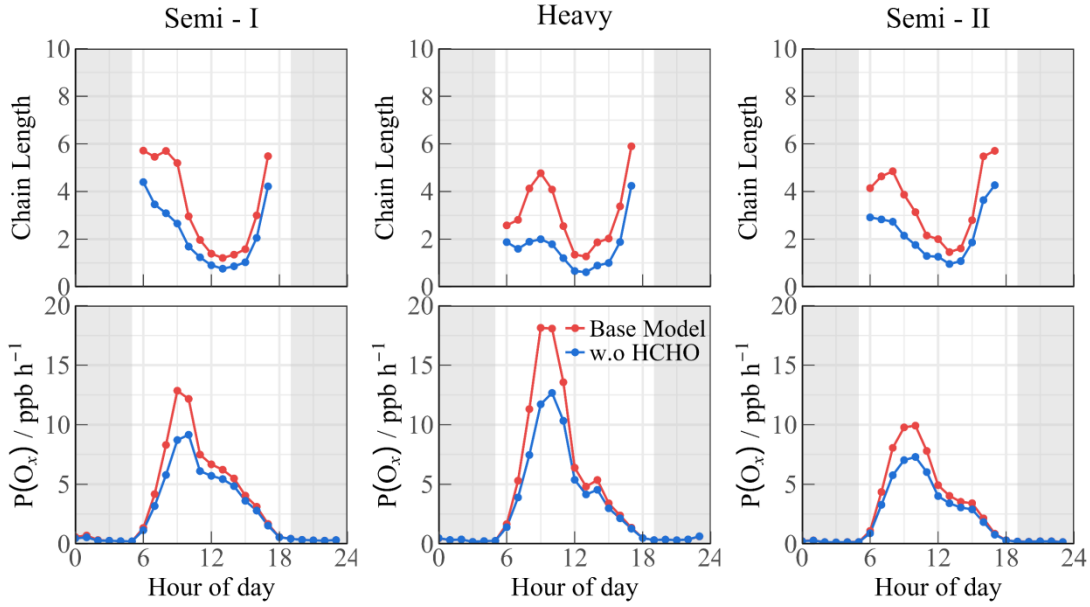

Fig. S8. The relationship between radical cycling and ozone pollution is established through chain length (ChL) and ozone production rate (P(Ox)). To test the influence of HCHO, its concentration was both constrained and unconstrained. The grey areas indicate nighttime periods.

Tables in supplementary material

Table.S1. Detailed information of supporting measurements.

Species	Methods	limit of detection	Accuracy (1 σ)	Time resolution
OH	LIF	3.3×10^5 cm^{-3}	±13%	60s
HO_2	LIF	1.1×10^6 cm^{-3}	±17%	60s
RO_2	LIF	2.6×10^6 cm^{-3}	±21%	60s
k_{OH}	LP-LIF	0.3 s^{-1}	±20%	180s
Temperature	Met One 083E	−50 to 50 °C	±0.5%	60s
Relative humidity	Met One 083E	0 − 100%	±2.0%	60s
WS	Met One 014A	0.45 − 60 m/s	± 0.11 m/s	1min
WD	Met One 024A	0−360° (>0.45 m/s)	±5°	1min
Pressure	Met One 092	600−1100 hPa	±0.5%	60s
J-values	SR	-	± 10%	60s
$PM_{2.5}$	TEOM	0.1 μg/m^3	± 10%	1h
O_3	UV	0.5 ppb	±10%	60s
	UV	0.4 ppb	±10%	60s
NO	CL	50 ppt	±10%	60s
NO_2	CL	50 ppt	±10%	60s
SO_2	UV-F	0.1 ppb	±10%	60s
CO	NDIR	50 ppb	±10%	60s
	CRDS	15 ppb	±10%	60s
PAN	GC-ECD	50 ppt	±10%	60s
HONO	CEAS	150 ppt	±15%	60s
HCHO	Hantzsch	200 ppt	±5%	60s
NMHCs	GC-MS/FID	5−70 ppt	± 10−15%	1h